

Van Doorne CVT Fluid Test: A Test Method on Belt-Pulley Level to Select Fluids for Push Belt CVT Applications

Bert Pennings, Mark van Drogen, Arjen Brandsma, Erik van Ginkel and Marlène Lemmens

Van Doorne's Transmissie b.v. / Bosch Group

Copyright © 2003 SAE International

ABSTRACT

Since the market for continuously variable transmissions (CVTs) is expanding rapidly and customer demands become more and more specific, there is an increasing need for adequate CVT fluids. In order to develop and apply new fluids, it is necessary to have reliable methods for fluid testing. However, test methods and standards that are being used nowadays for automatic transmission applications are not sufficient to select fluids for push belt CVT applications since they do not incorporate the belt-pulley behaviour. In this paper a method is described to test fluids on a belt-pulley level. The test method comprises full load testing in several ratios in which durability and functionality related push belt CVT items are being examined. This Van Doorne CVT Fluid Test can be used in addition to existing fluid tests in order to determine the suitability of fluids for push belt CVT applications.

1 INTRODUCTION

The market for belt type CVTs is rapidly growing. Since belt production start up at Van Doorne's Transmissie (VDT) in 1985, more than 5 million vehicles have been equipped with a push belt CVT. At this moment, more than 1.2 million push belt CVTs per year are being required for the Japanese, USA, European and Korean market. About 45 different vehicle models are currently available with push belt CVT. To further extend the application range of its push belt, VDT is examining more severe requirements regarding transmittable power, transmission size (centre distance), ratio coverage and durability. To meet those requirements, the power density of belt and pulley needs to be increased [1]. The current push belt status is nicely shown by the Nissan Murano with push belt CVT that has a ratio

coverage of 5.4 and can cope with a 3.5 liter V6 180 kW/350 Nm engine with torque convertor, applying drive side torque levels on the belt that lie above 500 Nm [2].

Further extension of the CVT application range can among other things be achieved by optimizing CVT fluids for given belt-pulley requirements. In order to develop and apply such new fluids it is necessary to have reliable methods for fluid testing. However the test methods and standards that are being used for automatic transmission applications are not sufficient to select fluids for push belt CVT applications, since they do not incorporate the belt-pulley behaviour. In addition to the well-known standardized tests concerning for example shear stability, foaming tendency or oxidation resistance, fluid testing is thus required at belt-pulley level. At VDT, a method has been developed to test fluids in the variator i.e. the belt-pulley system. Examples of a variator and a Van Doorne push belt are given in Figures 1.1 and 1.2.

The Van Doorne CVT Fluid Test should be regarded as a fluid screening test in which the relevant (variator) items for push belt CVT application are being examined. An actual approval of fluids for push belt CVT application will require additional validation tests at belt-boxes and at transmission level. However, the future perspective is a Van Doorne CVT Fluid Test that is suitable as variator validation test and that can be part of fluid standards for CVT applications like for instance the DEX-CVT[®] specification [3].

In this paper, a description is given of the fluid test items, test procedure, recommended values for test items and limitations. A justification for this test set-up is given as well as recommendations for further improvement.

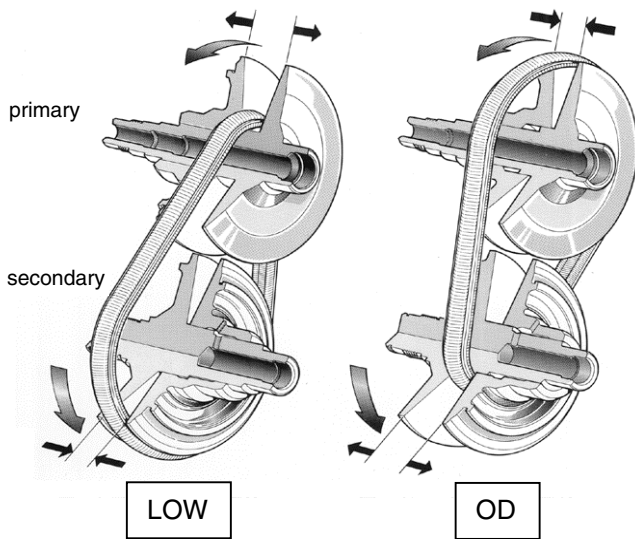


Figure 1.1 Example of a variator and its working principle; In the variator, power is being transmitted from the primary to the secondary pulley by means of friction between the push belt elements and the pulley sheaves. Stepless shifting between the extreme ratios LOW and OD is being realized by changing the pulley clamping forces through changing the axial position of the moveable pulley sheaves.

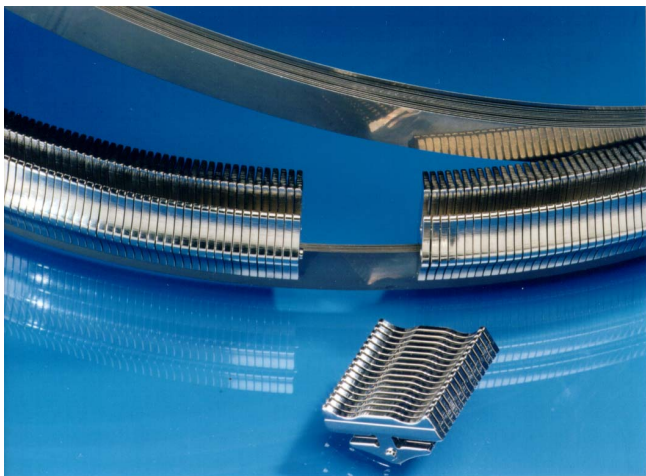


Figure 1.2 Example of a (partly disassembled) Van Doorne push belt with approximately 400 elements and 2 sets of 9 rings.

2 VAN DOORNE CVT FLUID TEST ITEMS

By testing CVT fluids at belt-pulley level all items, that are being considered as relevant for applying the push belt variator in CVTs, can be examined. These items can be classified as durability or functionality related items:

DURABILITY ITEMS

- wear of the belt and pulleys
- fatigue of the belt and pulleys
- degradation of the fluid

FUNCTIONALITY ITEMS

- maximum torque transmittance or torque capacity
- variator efficiency
- noise and vibrations
- cooling properties/heat dissipation

In Chapter 4 is described how CVT fluids can affect these items. How these items are addressed in the test procedure is presented in Chapter 3.

3 VAN DOORNE CVT FLUID TEST PROCEDURE

The fluid test procedure comprises 100 hours full load testing at nominal torque in three fixed ratios: 40 hrs TOP, 40 hrs OD and 20 hrs LOW ratio. LOW and OD are the two most extreme ratios of the variator, while TOP is the ratio where vehicle top-speed is being reached.

This durability cycle is being supplemented with wear inspections, wear measurements and functionality related measurements. All test results obtained for a fluid under investigation are being compared to results obtained with a reference fluid in order to judge the suitability of the fluid tested. ESSO EZL799 is currently being used as the reference fluid.

3.1 TEST EQUIPMENT

The fluid tests are being performed with VDT's 24 mm push belt type 901018 (24/9/1.5/208.8) and ZFST (P811/Alaska) pulleys, using VDT belt boxes and test rigs (see Figure 3.1).

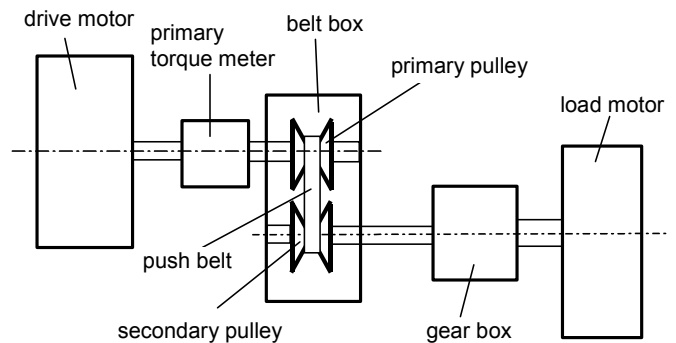


Figure 3.1 Test equipment (test rig and belt box)

A fluid sump volume of approximately 30-40 litres is being used. The tests are being performed with regular production belts and pulleys from one production batch in order to minimize variation in hardware. Whenever belts or pulleys from other production batches are being used, reference tests have to be performed with the reference fluid.

3.2 TEST PROCEDURE

The CVT fluids are being subjected to the test procedure as shown in Table 1.

Table 1 Van Doorne CVT Fluid Test procedure

Step	Action
1	Measurement of push belt ring roughness and element profile
2	40 hrs full load durability test in TOP ratio
3	Torque capacity measurement in TOP ratio
4	Belt inspection and fluid sampling
5	40 hrs full load durability test in OD ratio
6	Belt inspection and fluid sampling
7	15 hours half load and 20 hrs full load durability test in LOW ratio
8	Belt inspection, measurement of ring roughness, element profile and fluid sampling
9	Torque capacity measurement in OD ratio
10	Torque capacity measurement in OD ratio at elevated speed / decreased fluid temperature
11	Transition torque measurements in LOW ratio
12	Torque capacity measurement in LOW ratio
13	Rotational vibration sensitivity measurements
14	Pulley inspection
15	Evaluation of test results

Step 1

Fluid test preparations comprise push belt ring roughness measurements and element flank profile measurements. For the innermost rings no. 1 and 2, the roughness values are being measured at the inside and outside of the rings. For a relevant number of marked elements the flank profile depth is being measured.

Step 2-5-7

Fixed ratio durability tests are being carried out in the order TOP, OD and LOW. These tests are being performed at the settings given in Table 2 (see Appendix). Primary and secondary pulley pressures are being applied at which a theoretical safety factor S_f of 1.3 is achieved, assuming a coefficient of friction of 0.09 between belt and pulley. (The safety factor S_f is the ratio of the maximum transmittable torque and the nominal torque.)

The belt splash temperatures are being measured at the secondary pulley and are being maintained at $135(\pm 5)^\circ\text{C}$ during testing by adjusting the belt lubrication flow. A minimum belt lubrication flow of 1.5 litres/min is however being specified.

Step 4-6-8

The fixed ratio durability tests in TOP, OD and LOW are being supplemented with the collection of fluid samples and visual inspections of the belt in order to investigate belt wear developed in the successive ratios (see Section 4.1).

The final belt inspection after durability testing in LOW ratio is being supplemented with measurements of the ring roughness and element flank profiles. For the innermost rings no. 1 and 2, the roughness values are being measured at the inside and outside of the rings. For a relevant number of marked elements the flank profile depth is being measured.

Step 3-9-12

The torque capacity in OD and LOW ratio is being measured after the final belt inspection and ring roughness plus element profile measurements. However, the torque capacity in TOP ratio is being measured directly after the 40 hours TOP test in order to minimize the amount of assembly/disassembly work (in TOP ratio a mechanical stop is being used in the primary pulley). The torque capacity measurements are being performed at the speeds and pressures that are also applied for the durability tests (see Tables 2 and 3). These measurements consist of a controlled increase of the torque at which the belt slip rate is carefully being monitored. The torque capacity is the highest transmittable torque at which the measured slip rate is still stable. Once the slip rate becomes unstable the maximum transmittable torque is being exceeded (see Section 4.4).

Step 10

Additional torque capacity measurements are being performed in OD ratio to test the influence of an alternative primary speed (5300 rpm) and sump temperature (60°C) (see Table 3 in the Appendix).

Step 11

Transition torque measurements in LOW ratio are being performed at the settings given in Table 4 (see Appendix). These transition torques are indicative for the element saddle-ring friction that in turn influences ring stresses (see Section 4.2).

Step 13

In order to perform rotational vibration sensitivity measurements, the test rig assembly is being modified to a no-load situation (spin loss conditions) meaning disassembly of the secondary gear box and load motor. Furthermore an encoder is being installed to measure the rotational speed. The rotational vibrations are being derived by taking the derivatives of this signal. This data will be analysed performing a Fast Fourier Transform (FFT) analysis to separate the rotational vibrations into a frequency distribution.

The rotational vibration sensitivity test comprises eight measurements at various settings for the following factors of influence: rotational speed, pressure and temperature (see Section 4.6). In Table 5 the particular

settings for the vibration sensitivity measurements are presented.

Step 14

Visual inspection of the pulley wear is being performed according to a standard VDT inspection procedure which comprises visual inspection of several internal pulley contacts and belt-pulley contacts. The wear observed is being rated on the same scale as for belt wear (see Section 4.1).

Step 15

The test results obtained are being compared to results that are obtained with the reference fluid. Finally a judgement can be given concerning the suitability for push belt CVT application of the fluid tested.

4 JUSTIFICATION FOR CURRENT FLUID TEST PROCEDURE - RECOMMENDED VALUES - TEST IMPROVEMENTS

To secure proper functioning of the variator during lifetime of a vehicle, new applications are being released by means of Long Durability Cycles (LDCs). An LDC comprises 420 hours full load testing in three fixed ratios: 150 hrs TOP, 250 hrs OD and 20 hrs LOW ratio. This corresponds to circa 70,000 km (full load) testing which is less than the required vehicle lifetime (more than 250,000 km). However, the LDC test settings correspond to the most severe conditions that occur in the field (LOW and OD settings: maximum engine torque, smallest running radii; TOP settings: maximum engine power). This implies the most severe belt and pulley loading that will occur in the field in terms of contact pressures, contact speeds and stress levels in the components. The full load LDC is therefore being accepted as a test that secures variator durability in the field. Disadvantage of the LDC is the long test duration which makes the LDC less suitable for e.g. fluid screening purposes. In the Van Doorne CVT Fluid Test the same test settings are being applied as in the LDC. The test duration is however reduced substantially to only 100 hours which corresponds to approximately 17,000 km (full load) testing.

In the following sections it is shown that the Van Doorne CVT Fluid Test can secure to a large extent functionality items as well as durability items.

4.1 WEAR OF THE PUSH BELT AND PULLEYS

During the Van Doorne CVT Fluid Test, wear develops in all contact areas between belt and pulleys and in the internal push belt contacts. The most important items for visual inspection of belt and pulleys during the fluid test are summarised below and visualized in Figure 4.1.1.

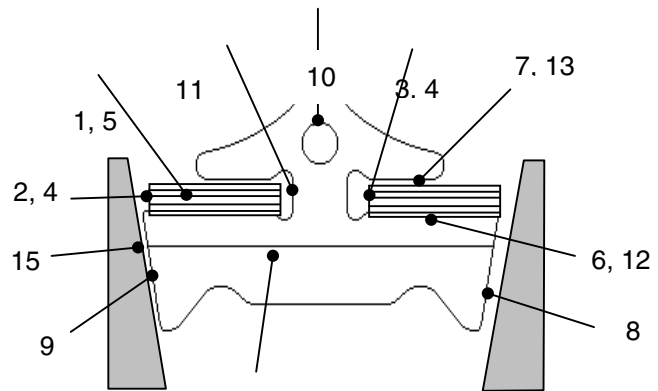


Figure 4.1.1 14 and pulley wear inspection items (internal belt contacts and belt-pulley contact areas).

Element-ring contacts: (1) elongation of the rings, (3) ring facet at element pillar side, (4) formation of burrs on the ring facet at element pillar side, (6) inner surface of ring no.1, (7) outer surface of ring no.9, (11) element pillar, (12) element saddle, (13) element ear.

Element-element contacts: (10) element dimple and hole, (14) element rocking edge.

Ring-ring contacts: (1) elongation of the rings, (5) inner and outer ring surfaces.

Pulley sheave-element contacts: (8, 9) element left and right flank, (15) sheave surfaces in the running tracks of TOP, OD, or LOW ratio.

Pulley sheave-ring contacts: (2) ring facet at sheave side, (4) formation of burrs on the ring facet at sheave side.

Wear in these contacts is an important fluid test item because it can influence variator durability and/or functionality as is shown with some examples: (1) The torque transmittance in the variator is among other things being determined by the element flank profile depth. This flank profile prevents separation of the belt and pulley by a large amount of fluid. Excessive wear of the element flank profile may cause such a fluid film which will lead to a drastic decrease of torque capacity. (2) Excessive wear of the element-element contacts dimple and hole increases the positioning freedom of the elements which can result in higher element stresses and even element (belt) failure. (3) Drastic changes of the surface roughness of the rings can affect internal belt friction and thereby ring stresses and ring fatigue durability (see also Section 4.2). (4) Excessive wear of the ring facets such as the formation of burrs can cause ring (belt) failures which is clearly unacceptable.

In general, wear is distinguished as *fatigue wear*, *adhesive wear*, *abrasive wear* and *tribochemical wear*, but often combinations of these wear types occur [4]. All mentioned wear types have been observed during visual inspections of belts and pulleys after LDCs. A

well known example of fatigue wear is pitting that is frequently present on element flanks, pulley sheaves and the inner surface of ring no.1. The smooth/uniform wear on the inner and outer ring surfaces and on the element saddles is probably caused by combinations of tribochemical and abrasive wear. When applied axial forces on the belt are insufficient (i.e. safety factor $S_f < 1$) belt slippage occurs, which can lead to adhesive wear on the element flanks and pulley sheaves.

In order to determine whether variator wear during the fluid test correlates with wear during an LDC, an assessment is made based on belt wear. For a significant number of LDCs (9x) and fluid tests (6x) that was performed with VDT's reference fluid, belt wear was examined according VDT's standard belt inspection procedure. This comprises visual inspections of all individual rings and of a relevant number of elements. The wear observed is being rated on a scale from 0 to 6 meaning "no wear" {0}, "light wear" {2}, "moderate wear" {4} and "heavy wear" {6}. Additional comments are being made when specific wear types as mentioned before are being observed.

Results of the belt inspections are shown in Figures 4.1.2 and 4.1.3. In these figures, average wear levels per inspection item for the fluid tests and LDCs are shown. The question whether the wear levels for the fluid test and the LDC have equal averages, is investigated with standard statistical techniques. One straightforward approach uses a parametric Student *t*-test, assuming wear levels for all inspection items to be normally distributed. This is a reasonable assumption; however, the Student *t*-test requires equal variances and this was shown to be not the case, using a standard *F*-test.

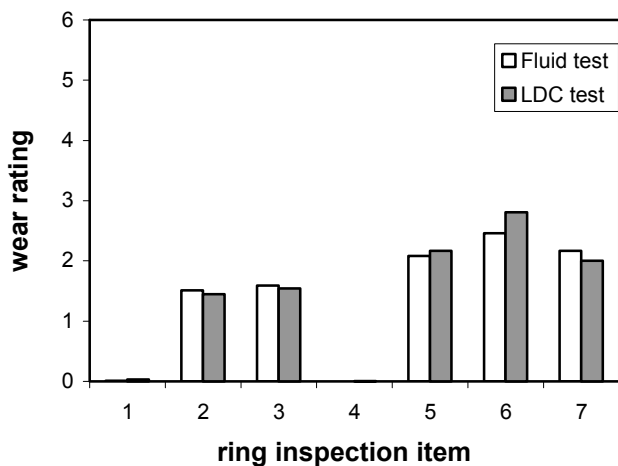


Figure 4.1.2 Ring wear during fluid test and LDC (average wear levels per inspection item).

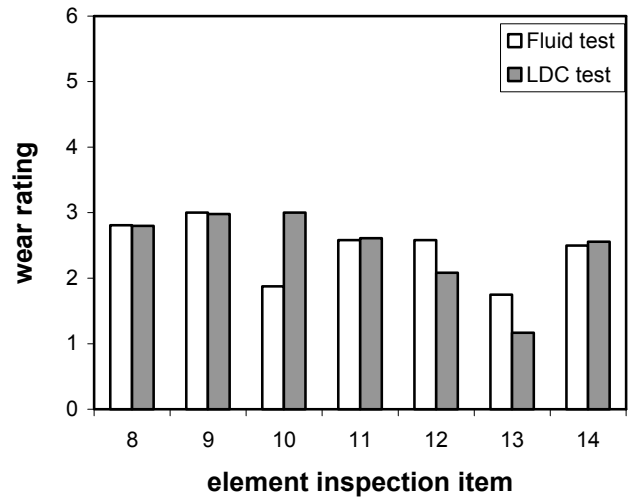


Figure 4.1.3 Element wear during fluid test and LDC (average wear levels per inspection item).

Therefore a non-parametric test is applied for which no further assumptions are necessary for the variance or distribution of the wear levels. From this Kruskal-Wallis test [5], it follows that given a significance level of 5% only for inspection items 10 and 13 the average wear during fluid test and LDC is not equal. For item 10 (element dimple and hole) wear is somewhat less after the fluid test compared to the LDC. For item 13 (element ear) wear appears to be slightly higher after the fluid test compared to the LDC, but this is not easy to understand or to clarify. It can be concluded that for all other items, the average wear during fluid test and LDC is equal.

A specific feature of belt wear that can easily be measured is the belt endplay that develops during belt durability tests. This endplay is the summation of the play (or clearance) between all individual elements in the push belt. The change of this endplay is a result of the wear of the elements rocking edge and the elongation of the rings. The change of belt endplay was measured during the belt inspections of the fluid tests (6x) and LDCs (9x) mentioned above. The average values obtained are shown in Figure 4.1.4. What can be seen is that the major part of the increase in endplay during the fluid test develops during the 40 hours TOP. For an LDC this is also the case: the major part of the increase of endplay develops during the 150 hours TOP. By applying the same statistical techniques as used above, it can be shown that the final average endplay due to the fluid test does not differ significantly from the average endplay that develops during an LDC. These results are in agreement with the visual inspections (Figures 4.1.2 and 4.1.3) and confirm that the wear levels during the Van Doorne CVT Fluid Test are comparable to the wear during an LDC.

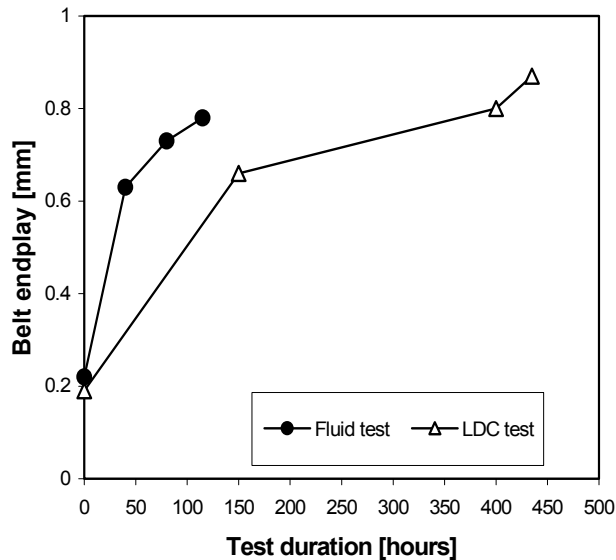


Figure 4.1.4 Change of belt endplay during fluid test and LDC (endplay after TOP, OD and LOW).

Based on the reference fluid tests, recommended values can be given for belt and pulley wear during the Van Doorne CVT Fluid Test. For all belt and pulley inspection items, it is recommended that wear ≤ 4 (on mentioned scale from 0–6). For belt endplay it is recommended that the *increase* during the fluid test is ≤ 0.8 mm. When a fluid meets these recommended values after the Van Doorne CVT Fluid Test it may be expected that the wear after an LDC will also be acceptable and the variator will still perform adequately, provided that the other fluid test items also meet the recommendations.

Among the fluids that were received so far from lubricant developers or OEMs and that were tested at VDT there are however no clear examples of fluids that were judged unsuitable for push belt CVT applications solely because of belt and/or pulley wear.

Future perspective is to add more objective wear data to the current visual belt and pulley inspections. Therefore ring roughness and element flank profile changes are already being monitored in the fluid tests. For the innermost rings no.1 and rings no.2 the roughness values are being measured at the inside and outside of the rings. For a relevant number of marked elements the flank profile depth is being measured. Both visual inspections and wear measurements are being performed prior to most of the functional measurements (torque capacity, transition torque). Any wear or damage introduced during these functional measurements is now excluded from the inspections and wear measurements.

4.2 FATIGUE OF THE PUSH BELT AND PULLEYS

During operation of the variator, the push belt and pulleys are being subjected to cyclic loading which may lead to fatigue. This section deals with the influence of the fluid choice to fatigue of belt and pulleys.

Fatigue at the interface of contacting bodies may lead to wear of the interacting surfaces and therefore this type of fatigue is addressed in Section 4.1.

The push belt rings are being subjected to bending stresses, tensile stresses, contact stresses and friction related stresses. The bending stresses are determined by applied running radii (ratio) and ring thickness. It is not likely that the applied fluids will have an influence on the bending stress magnitudes. The tensile stresses are mainly determined by applied clamping forces (pressures, centrifugal forces, spring forces), rotational speeds and torque levels. The required clamping forces are depending on the element sheave friction assuming a constant safety factor. The influence of the fluid to element sheave friction with recommended values is presented in Section 4.4. The stress levels in elements and pulley are also being determined by the applied clamping forces, again depending on the element sheave friction.

The contact and relative motion between the element saddles and the innermost rings and between the rings (see Figure 4.1.1) will cause frictional forces on these rings. These frictional forces may affect the (amplitude of the) tensile stresses and hence influence the fatigue life/durability of the rings.

The magnitude of these frictional forces at certain test settings (e.g. normal forces acting on the rings) can be characterised by the element saddle-ring and the ring-ring coefficient of friction, respectively μ_{er} and μ_{rr} and may substantially be influenced by the applied fluid. Instead of performing durability tests, a functional and reduced test is being preferred. Therefore functional friction tests are being carried out during the fluid test as an indication of the possible durability of the fluid candidate.

Element saddle-ring coefficients of friction can be determined at the test rig described in Section 3.1, by carefully measuring the so-called transition torque in LOW ratio. Measurement of this transition torque consists of a controlled increase of the torque at which the belt slip rate is carefully being monitored. The situation is being represented in a so-called slip curve as shown in Figure 4.2.1.

On the horizontal axis of the slip curve the primary or input torque T_{prim} is denoted and on the vertical axis the slip rate. The slip rate [%] is defined as

$$\text{slip rate} = \frac{i_{\text{speed}} - i_{\text{spinloss}}}{i_{\text{spinloss}}} \cdot 100\%, \quad (1)$$

where $i_{\text{speed}} = \frac{n_{\text{prim}}}{n_{\text{sec}}}$ and i_{spinloss} equals the initial i_{speed} at the no-load condition (spin loss).

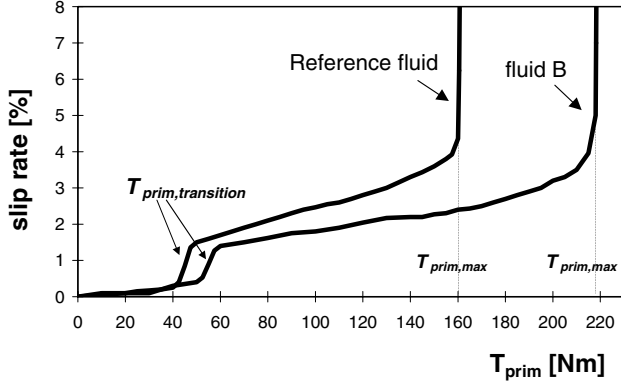


Figure 4.2.1 Slip curve measurements with transition torque in LOW for the reference fluid and fluid B

At the variator test rig the output torque T_{sec} will be adjusted and a feed forward action is being used to adjust the input torque T_{prim} keeping the primary rotational speed at a constant value. It is customary at VDT that T_{prim} is labelled instead of T_{sec} .

The transition torque $T_{\text{prim,transition}}$ is the torque level at which the slip rate suddenly increases. At the transition point the compression side and the slack side exchange sides [6]. This means that the element compression force $F_{\text{compr,element}}$ at this torque equals zero. This can be explained by considering force equilibrium of one pulley and belt part. The element compression force $F_{\text{compr,element}}$ balances the applied torque T_{prim} at running radius R_{prim} and the resulting tensile ring force $\Delta F_{\text{tens,ring}}$ (depending on e.g. μ_{er}) according to

$$F_{\text{compr,element}} - \Delta F_{\text{tens,ring}} + \frac{T_{\text{prim}}}{R_{\text{prim}}} = 0. \quad (2)$$

From Eq. (2) it can be seen that at increasing T_{prim} starting from 0 Nm, $F_{\text{compr,element}}$ changes sign for a certain T_{prim} ($\equiv T_{\text{prim,transition}}$), which means the compression side will become the slack side and vice versa.

The value for this transition torque is being used to calculate the element saddle-ring coefficient of friction μ_{er} by solving the set of governing equations [7]. Since $T_{\text{prim}} (= T_{\text{prim,transition}})$, $F_{\text{compr,element}} (= 0)$ and the clamping forces (pressures) are known, the set of equations can be solved resulting in a value for the μ_{er} . This concerns the kinetic μ_{er} since all elements are slipping relative to the inner surface of ring no.1.

In Table 4 (see Appendix) the settings for the transition torque measurements in LOW are presented. Next to the measurement at the standard setting in LOW for the normal durability test according to Table 2 ($n_{\text{prim}} = 4000$ rpm and sump temperature equals 100°C), additional tests are being carried out at different settings in order to get a more complete picture of the frictional properties of the element saddle-ring contact.

In Figure 4.2.2 transition torque measurements for several fluids are shown, determined at the standard LOW settings. μ_{er} measurements by means of the transition torque method is also illustrated in Figure 4.6.5 for a large range of factors of influence (e.g. velocity, pressure, temperature/viscosity, surface roughness) using VDT's reference fluid.

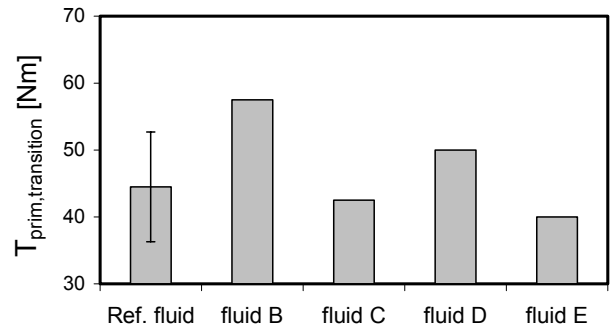


Figure 4.2.2 Transition torque measurements in LOW for several fluids

The transition torque is proportional to the saddle-ring coefficient of friction. Therefore a higher transition torque results in higher frictional forces acting on the innermost rings. These frictional forces should be added to the bending stresses and tensile stresses. Based on the previous, it is therefore likely that applied fluids will influence the loading conditions of the innermost rings and thereby influence ring and push belt durability.

The contact and relative velocity between individual rings will also cause frictional forces acting on the rings. The magnitude of these frictional forces at certain test settings is being determined by the ring-ring coefficient of friction μ_{rr} that may in turn substantially be influenced by the applied fluids. However, measurement of these ring-ring coefficients of friction in the variator would require severe modifications or even the use of a dedicated test rig. Therefore the evaluation of the ring-ring coefficient of friction is not included in the current fluid test. The importance of ring-ring frictional forces given the influence on ring loading conditions and ring durability is however clear. Additional ring-ring friction measurements are therefore being considered as an improvement of the current fluid test.

The recommended value for $T_{prim,transition}$ is derived based on the average values and 3σ -intervals obtained during the reference fluid tests. For a *single* Van Doorne CVT Fluid Test the following maximum values are being allowed:

LOW ratio: $T_{prim,transition} \leq 53 \text{ Nm}$

When a fluid does not meet this recommendation it may be expected that the $T_{prim,transition}$ is significantly higher than for VDT's reference fluid which is assumed to have a negative effect on belt durability. It should be stressed that the value mentioned above is valid for the hardware and test settings as described in Chapter 3. Other values may be suitable for other hardware/settings.

However, some fluids show besides a higher $T_{prim,transition}$ also a higher $T_{prim,max}$ (see e.g. Figure 4.2.1). In this case it is possible to apply lower clamping forces in the CVT-design. This will influence the ring stresses to a certain extent and a higher $T_{prim,transition}$ may be allowed.

4.3 DEGRADATION OF THE FLUID

Degradation of CVT fluids during variator operation may affect wear and fatigue of the belt and/or pulleys as well as functionality related items. Fluid degradation should therefore be considered as a potentially relevant fluid test item.

It is presumed that fluid degradation depends on e.g. fluid sump volume, fluid sump temperature, belt splash temperature and test duration. Belt (durability) tests at VDT are usually being performed at sump temperatures of about 70-80°C. However, during the Van Doorne CVT Fluid Test a fluid sump temperature of 100°C and a belt splash temperature of 135(±5)°C are being maintained in an attempt to accelerate fluid degradation. The belt splash temperature has to be limited at 135(±5)°C, since higher temperatures may result in a tempering effect of the elements (i.e. hardness decrease) which may influence for example element wear.

Current sump volumes during fluid tests are approximately 30-40 litres. Further reduction of sump volumes will probably result in higher fluid loading and may accelerate degradation. The future perspective is to use sump volumes of only a few litres.

The fluid sampling that is being performed after the durability tests in TOP, OD and LOW offers the possibility to determine whether certain specific chemical and/or physical fluid properties have changed during the fluid test.

However, at the moment there are no indications that wear, fatigue and functionality related items after an LDC differ from the fluid test as a result of a difference in fluid degradation.

4.4 MAXIMUM TORQUE TRANSMITTANCE OR TORQUE CAPACITY

In the variator, torque or power is being transmitted from the primary to the secondary pulley by means of friction between the push belt elements and pulley sheaves. For safe variator operation i.e. preventing belt slippage, clamping forces F_{ax} according to the so-called clamping force equations (3) and (4), are required at both the primary and the secondary pulley.

$$F_{ax,prim} = \frac{T_{prim} \cdot S_f \cdot \cos \lambda}{2 \cdot R_{prim} \cdot \mu_{es}} \quad (3)$$

$$F_{ax,sec} = \frac{T_{sec} \cdot S_f \cdot \cos \lambda}{2 \cdot R_{sec} \cdot \mu_{es}} \quad (4)$$

where T_{prim} and T_{sec} are respectively the primary torque and the secondary torque, S_f is the safety factor and λ is the cone angle. R_{prim} and R_{sec} represent respectively the primary running radius and the secondary running radius and μ_{es} is the coefficient of friction for the element-sheave contact.

As described in Section 3.2, primary and secondary clamping forces are being applied for the fixed ratio durability tests at which a theoretical safety factor $S_f=1.3$ is being achieved assuming $\mu_{es}=0.09$. During the torque capacity measurements, the maximum transmittable torque $T_{prim,max}$ is being measured at the primary pulley (see also Figure 4.2.1). This $T_{prim,max}$ occurs at $S_f \equiv 1$ and with known $F_{ax,prim}$, R_{prim} and $\lambda=11^\circ$ the μ_{es} can be calculated using Eq.(3). In LOW ratio, belt slippage at maximum transmittable torque will indeed occur at the primary pulley and Eq.(3) is being used to calculate μ_{es} at which in practice it is being supposed that $F_{ax,prim} \cong F_{ax,sec}$. However, in TOP and OD belt slippage will occur at the secondary pulley. The μ_{es} is then being calculated at the secondary pulley using Eq.(4) with $F_{ax,sec}$ and assuming that $T_{prim,max}/R_{prim} = T_{sec,max}/R_{sec}$.

The μ_{es} is being influenced by the applied CVT fluids. Fluids that cause low torque capacity (i.e. low μ_{es}) will require higher clamping forces for safe variator operation. Unfortunately this will result in higher loading of the variator (e.g. increase of ring tensile stresses) with disadvantageous consequences for the design of belt, pulleys, variator actuation, et cetera.

Power losses will increase and variator efficiency will consequently decrease. Fluids that cause high torque capacity (i.e. high μ_{es}) obviously give the opportunity to apply smaller clamping forces. Measurement of torque capacity therefore gives valuable information about the suitability of fluids for push belt CVT application.

During five Van Doorne CVT Fluid Tests with VDT's reference fluid, $T_{prim,max}$ was measured in the ratios TOP, OD and LOW according to the test procedure (see Section 3.2) and the corresponding values for μ_{es} were determined. Figure 4.4.1 shows the torque levels $T_{prim,nominal}$ that are applied during the durability tests (see also Table 2) as well as the average values that were obtained for $T_{prim,max}$ including error bars representing 3σ -intervals. Figure 4.4.2 shows the average values for μ_{es} including error bars representing 3σ -intervals. These values are comparable to values for μ_{es} that are obtained after LDCs with VDT's reference fluid.

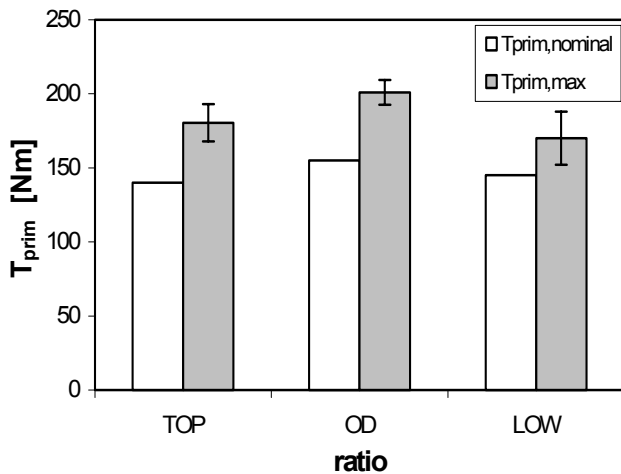


Figure 4.4.1 $T_{prim,nominal}$ and $T_{prim,max}$ in ratios TOP, OD and LOW during fluid tests with the reference fluid.

As mentioned in Section 3.2, the torque capacity measurements in OD and LOW ratio are being performed after completing the 100 hours full load testing, final belt inspection and ring roughness plus element profile measurements. The belt wear that is observed at final belt inspection and the ring roughness plus element profile are therefore not influenced by these torque capacity measurements. The single torque capacity measurement in TOP ratio is being performed directly after the 40 hours TOP test in order to minimise the amount of assembly/disassembly work (in TOP ratio a mechanical stop is being used in the primary pulley). Experiments in which the torque capacity measurement in TOP was repeated up to ten times did not show a measurable decrease of $T_{prim,max}$ and μ_{es} . Also no additional belt/pulley wear was observed at visual inspections in between the ten torque capacity

measurements. Therefore, the influence of this torque capacity measurement on belt/pulley wear and functional behaviour in OD and LOW is being expected to be negligible which justifies the current test procedure.

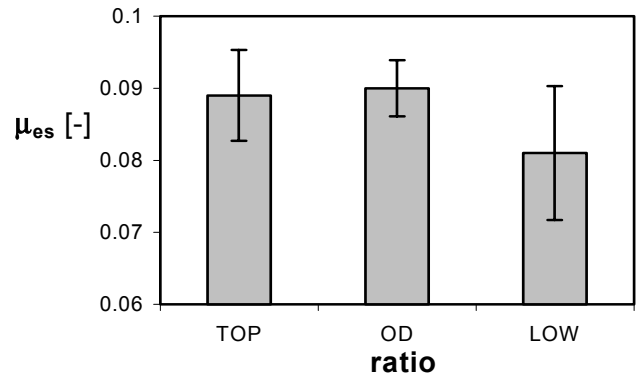


Figure 4.4.2 Coefficients of friction element-sheave μ_{es} in ratios TOP, OD and LOW during fluid tests with the reference fluid.

Some results of single fluid tests that were performed with fluids received from lubricant developers or OEMs are shown in Figure 4.4.3. Also shown are the average values for μ_{es} with 3σ -intervals that were obtained during the reference tests. In case of Fluid B, significantly higher values for $T_{prim,max}$ and μ_{es} were obtained in all test ratios compared to the reference fluid ESSO EZL799. In case of Fluid C significantly lower values for $T_{prim,max}$ and μ_{es} were obtained in TOP and OD. (The assumption is that values obtained with fluid B and C are also normally distributed with the same standard deviations σ as for the reference fluid.)

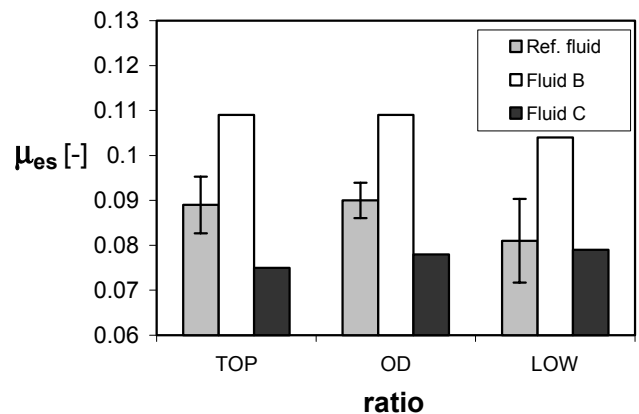


Figure 4.4.3 Coefficients of friction element-sheave μ_{es} in ratios TOP, OD and LOW during fluid tests with several fluids.

The recommended values are derived for $T_{prim,max}$ and μ_{es} , based on the average values and 3σ -intervals obtained during the reference fluid tests. For a *single* Van Doorne CVT Fluid Test the following minimum values are being required:

TOP ratio: $T_{prim,max} \geq 168 \text{ Nm}$, $\mu_{es} \geq 0.083$

OD ratio: $T_{prim,max} \geq 193 \text{ Nm}$, $\mu_{es} \geq 0.086$

LOW ratio: $T_{prim,max} \geq 152 \text{ Nm}$, $\mu_{es} \geq 0.072$

When a fluid does not meet these recommendations, it can be expected that the torque capacity and μ_{es} are significantly lower than for VDT's reference fluid. Fluids with lower values for $T_{prim,max}$ and μ_{es} will require adapted clamping forces for safe variator operation resulting in mentioned negative influences on variator durability and efficiency. Furthermore it should be stressed that the values mentioned above are valid for the hardware and test settings as described in Chapter 3. Other values may be suitable for other hardware/settings.

Future perspective: the test procedure might be changed/simplified in the future to 40-80 hours OD plus 20 hours LOW i.e. leaving out the 40 hours TOP test or replacing it by 40 hours additional OD. Therefore the torque capacity measurements in OD ratio at a primary speed of 5300 rpm (simulating TOP settings) are being introduced in the current CVT fluid test to determine the possible influence of belt speed on $T_{prim,max}$ and μ_{es} .

The torque capacity measurements in OD ratio at a sump temperature of 60°C are being introduced in the CVT fluid test to determine the possible influence of fluid temperature on $T_{prim,max}$ and μ_{es} . The results to be obtained may justify the addition of more functional testing at other sump temperatures to the current fluid test procedure.

4.5 VARIATOR EFFICIENCY

Variator efficiency is among other things being determined by the frictional losses in the belt-pulley contacts and internal belt contacts. Variator efficiency thus depends on the coefficients of friction in these contacts that are in turn being influenced by the applied CVT fluids. Efficiency should therefore be considered as a potentially relevant fluid test item. Measurement of efficiency with the current fluid test equipment is however not accurate enough to distinguish (small) differences for different fluids. Therefore measurement of the coefficients of friction may be regarded as indicative for efficiency. High values for μ_{es} give the opportunity to apply smaller clamping forces which is beneficial for efficiency. Low values for μ_{er} (element saddle-ring) and μ_{rr} (ring-ring) are also beneficial since this reduces internal belt losses. These goals are in accordance with Sections 4.2 and 4.4.

4.6 NOISE AND VIBRATIONS

The variator noise levels are largely outside the audible domain. The reason for this is because the thickness of the elements in the push belt is small and therefore the element running frequency is high (as compared to e.g. the chain CVT). Furthermore it may be assumed that the choice of fluid has no effect and therefore variator noise will not be taken into account in the test procedure.

In transmissions gear rattle is sometimes being experienced. Gear rattle is being caused by rotational vibrations that arise from frictional behaviour in certain engineering parts such as clutches (i.e. shudder). There is also a relation between rotational vibrations as observed in the variator of a CVT and gear rattle. The accompanied term for this phenomenon is 'scratch' [8]. Fluid characteristics are believed to play a major role in the rotational vibration sensitivity of the variator [9]. Therefore an additional measurement procedure has been set up in the Van Doorne CVT Fluid Test to evaluate fluids with regard to their rotational vibration sensitivity.

4.6.1 Variator rotational vibration sensitivity

In some CVT designs, disturbing noises are being observed in the transfer gears between the secondary pulley set and the differential at certain operational conditions in LOW ratio [8]. These noises are caused by rattling of the gear teeth. This so-called gear rattle is a result of the fact that rotational vibrations (in terms of certain amplitudes and frequencies), which are superimposed onto the input speed of the gears, do not match with the driveline characteristics (e.g. mass, stiffness, damping) of the gear box to avoid this phenomenon [10].

Rotational vibrations in the variator at certain operational conditions can play a role in the occurrence of gear rattle depending on the driveline dynamics of a certain CVT design. Rotational vibrations in the variator originate from dynamic frictional behaviour in the contact between the saddle of the element and inner surface of ring no.1, the so-called element saddle-ring contact (see Figure 4.1.1). Exchanging ring sets with different wear levels in belts shows evidence of the influence of this particular contact to the occurrence of scratch.

Dynamical frictional behaviour, which may lead to vibrations due to a change in coefficient of friction with relative velocity, can be subdivided in [11]

- a. 'Classical' stick-slip, where the coefficient of friction changes when going from static to kinetic friction.

- b. Stick-slip-related or μ_k - V_r dependent behaviour, where in a system that is already in relative motion the kinetic coefficient of friction μ_k changes with relative velocity V_r .

a. Classical stick-slip

Classical stick-slip can arise when the coefficient of static friction μ_s is greater than the coefficient of kinetic friction μ_k . Consider Figure 4.6.1; the block with mass m will stick to the lower surface if the coefficient of friction is sufficiently large at the equilibrium position when moving it along with an absolute velocity of value $\dot{x} = V$. During the stick period the force relationship may be written as

$$cV + kx < \mu_s F_N. \quad (5)$$

During the stick phase, the spring force increases with time at a rate kVt (or kx) as the slider is displaced from point A to point B as shown in Figure 4.6.2. Up to point B, the static friction force is capable of withstanding the combined restoring forces consisting of the constant damping force cV and the increasing spring force kx . At point B, the restoring forces overcome the static friction force $\mu_s F_N$ and slip occurs to point C [11]. From this point the static friction force is again larger than the restoring forces and hence the stick phase is again present. The sequence as described above will now be repeated from A.

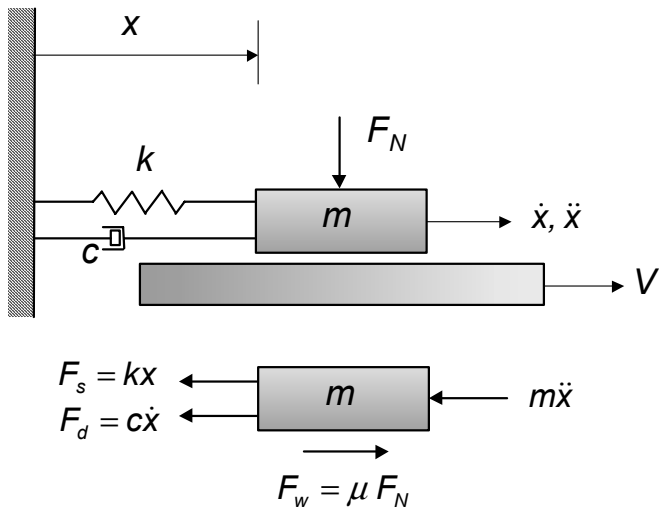


Figure 4.6.1 Mass-spring-damper-friction system and force equilibrium [11]

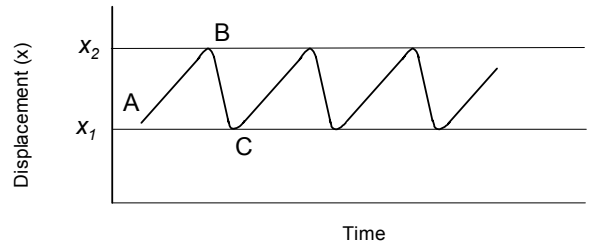


Figure 4.6.2 Displacement of block as a function of time during classical stick-slip behaviour [11]

b. μ_k - V_r dependent behaviour

In the slip phase, the motion of the body (mass) in Figure 4.6.1 can be described by the equation

$$m\ddot{x} + c\dot{x} + kx = \mu_k F_N. \quad (6)$$

It can be assumed that at a certain moment μ_k decreases with increasing relative velocity V_r according to hydrodynamic action and/or additive effects in the lubricated contact (for more information see the discussion about the Stribeck curve in the next section).

As a first approximation the dependence of μ_k on V_r can be modelled by a linear relationship with a certain negative slope ($\alpha < 0$) according to

$$\mu_k = \mu_k^0 + \alpha V_r. \quad (7)$$

The expression (7) for μ_k can be substituted in Eq. (6). With

$$V_r = V - \dot{x} \quad (8)$$

this yields the following equation

$$m\ddot{x} + (c + \alpha F_N)\dot{x} + kx = (\mu_k^0 + \alpha V) F_N. \quad (9)$$

Important to note is that the slope α has appeared in the damping term and in case of $\alpha < 0$ it acts in a negative way. A decreasing damping coefficient feeds energy into the system and makes vibrations and even resonance possible.

To illustrate the fact that a negative slope α may cause vibrations a dimensionless damping factor κ can be defined as

$$\kappa = \frac{c + \alpha F_N}{2\sqrt{mk}}. \quad (10)$$

Solving Eq.(9), it is possible to distinguish the following situations with regard to κ :

1. $\kappa > 1$ (case **a**) : *overdamped*. No oscillations are present and motion decays so that x approached the particular solution x_p for large values of time t .
2. $\kappa < 1$: *underdamped*. Oscillations occur. For
 - $0 < \kappa < 1$ (case **b**): vibration decays harmonically
 - $-1 < \kappa < 0$ (case **c**): vibration increases harmonically
 - $\kappa < -1$ (case **d**): vibration increases exponentially

In Figure 4.6.3 the effect of different values for α and hence also of κ on displacement x is shown for the cases **a-d**. As boundary conditions a very small initial displacement δ as disturbance to excite the system, a zero starting velocity \dot{x} and the particular solution $x_p = [(\mu_k^0 + \alpha V) F_N] / k$ are being used. From Eq. (10) and Figure 4.6.3 it can clearly be seen that the slope α in the μ/V_r curve (or Stribeck curve, see next section) plays an important role with regard to the vibration mode.

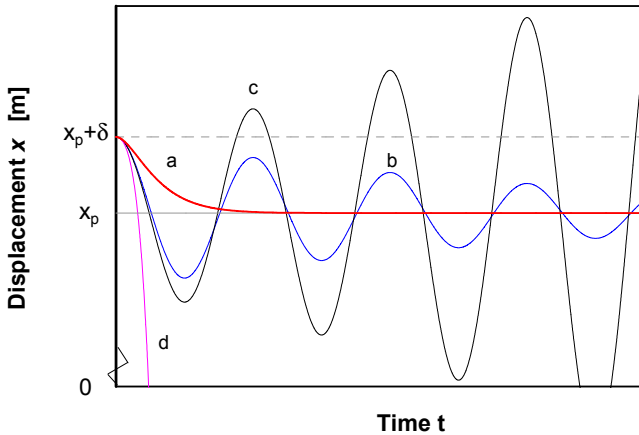


Figure 4.6.3 Displacement x in time for different values for κ (i.e. cases a-d)

This also shows that, unlike what quite often is assumed, stick is not a necessary condition for the occurrence of rotational vibrations, but that the behaviour of the change in coefficient of friction with velocity may lead to these vibrations. Furthermore it should be noticed that any disturbance (in the transmission) can lead to excitation of the mass-spring-damper-friction system due to the inherent unstable nature of this system.

4.6.2 Push belt and stick-slip phenomena

The mass-spring-damper-friction model will now be applied to the push belt and variator. The rotational vibrations are being experienced in LOW ratio so that this situation will be regarded here and the measurements will also be carried out in Low ratio. In LOW ratio it can be assumed that full (macro) slip will occur in the frictional contact between the saddles of the elements and the inner surface of ring no.1 at the

primary side, characterized by the relative velocity V_r . On the secondary side only creep between saddle and ring is being assumed [7].

In Figure 4.6.4 a simplified variator model representation is shown. In the dynamical system of the variator only relative motion between saddle and ring (as source) and vibrations of the secondary axis in the variator (as effect) are being considered, the rest will be assumed to be motionless in this case.

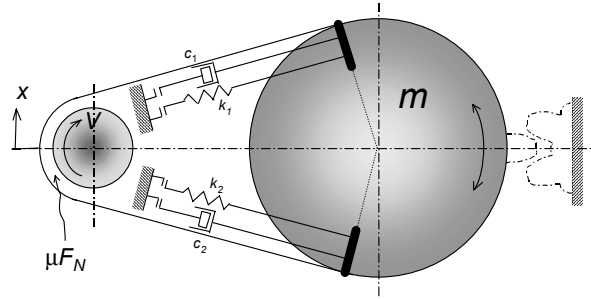


Figure 4.6.4 Simplified variator model

The (vibrating) mass in this model represents the secondary pulley/shaft in the variator. The element string between the primary and secondary pulley constitutes the spring when the stiffness is being considered and also plays a damping role. Two situations can be distinguished regarding the element string. The first is that the element string is not loaded in a way that compressive forces are able to overcome the clearance/endplay (the so-called 'slack' side). The second situation is when there is no clearance/endplay (the 'compression' side) in the element string anymore. According to the first situation, when there is some amount of clearance/endplay in the element string, this part does not have to be taken into account. However in the second situation, when there is no endplay, this part (with its characteristic stiffness and damping) has to be considered in the model.

The ring is moving relatively to the elements in the primary pulley with a certain relative velocity V . The overall relative velocity V_r (i.e. V superimposed with vibration \dot{x}), which is crucial for the frictional behaviour, is according to Eq.(8). The normal force in this contact is the parameter F_N used in the model. In this model only the frictional contact saddle-ring on the primary side is taken into account. The coefficient of friction in the element saddle-ring contact is being labeled as μ_{er} .

The dynamic behaviour of the coefficient of friction μ_{er} can be represented in the so-called Stribeck curve [12]. In this curve the coefficient of friction is being mapped as a function of the relative velocity V_r in the contact. To have a more complete picture of the frictional behaviour as well as to map certain

lubrication regimes, parameters as dynamic viscosity η_0 , average Hertzian pressure p_{av} and the combined surface roughness R_a' have to be taken into account (temperature effects will be incorporated in the viscosity). Therefore a dimensionless lubrication number L has been defined as [12]

$$L = \frac{V_r \eta_0}{p_{av} R_a'} \quad (11)$$

where the combined surface roughness R_a' is being determined by

$$R_a' = \sqrt{R_{a,saddle}^2 + R_{a,ring}^2} \quad (12)$$

Results of frictional measurements, performed at variator level in LOW ratio by means of the transition torque method (see Sections 3.2 and 4.2), are shown in Figure 4.6.5. The measurements have been carried out with the reference fluid at various operating conditions. These measurements clearly indicate the influence of the governing L -parameter in the resulting Stribeck curve. It is now possible to distinguish three lubrication regimes [12]:

1. Boundary lubrication (BL): shear takes place in the boundary layers of the contacting surfaces
2. Mixed lubrication (ML): mixed form of BL and EHL
3. (Elasto) hydrodynamic lubrication (EHL): shear takes place in the lubricant film

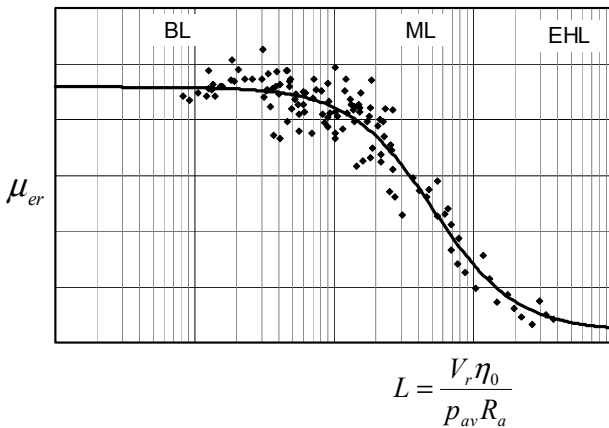


Figure 4.6.5 Stribeck curve measurements for element saddle-ring contact

Two effects, hydrodynamic action and additive behaviour determine the behaviour of μ against V_r or L and thus the value of the actual slope α . The hydrodynamic action [11] can be characterised by the hydrodynamic separation (i.e. resulting fluid film thickness over roughness). An increase in fluid film thickness will lead to a decrease in the coefficient of friction resulting into the transition from BL to ML and

eventually to EHL, depending on the roughness values. From the fluid's viewpoint, the viscosity is the property that influences the hydrodynamic action (i.e. higher viscosity results in larger separation).

Furthermore the wear and hence the resulting roughness value is being determined by the fluid's additive anti-wear properties at the governing operational conditions. The additives also determine the behaviour and the level of the coefficient of friction in the boundary lubrication regime (and strictly speaking in the mixed lubrication regime as well).

The factors of influence mentioned above are reflected in the rotational vibration sensitivity measurement settings as shown in Table 5 (see Appendix). The relative velocity V_r is being varied by means of a change in the rotational speed n_{prim} and the viscosity η_0 is inversely proportional to the temperature. The change in roughness is being taken into account by means of the wear of the contacting surfaces. The contact pressure is being varied by means of the hydraulic pressures in pulleys. In the next section the rotational vibration measurement results will be discussed.

4.6.3 Analysis of measurement results

Rotational vibrations in the frequency range between 0 and 250 Hz are being measured. This is the frequency range of interest for scratch according to the experience of OEMs. The rotational vibrations are presented in terms of the maximum acceleration amplitude in rad/s^2 per measurement. The maximum amplitude of each separate rotational vibration measurement contributes to a rotational vibration performance number. Several test runs have been performed with the reference fluid and three other CVT fluids as shown in Figure 4.6.6. Furthermore the repeatability of the test is being indicated by the minimum and maximum values of the tests. A high rotational vibration performance number indicates that the fluid is more susceptible to scratch in a scratch sensitive transmission.

4.6.4 Justification – test improvements

Rotational vibration levels obtained during these tests have been compared with scratch tests of several OEMs for some transmission designs that are sensitive for gear rattle and correlations for the different test conditions are being demonstrated. OEMs' scratch testing methods range from subjective noise rating methods by sound panels to (rotational) vibration measurements on vehicle, transmission and variator level.

However, no single correlation can be made for different transmission designs due to different dynamical driveline characteristics. Therefore no criterion in terms of a maximum rotational vibration level can be given at certain test settings. Only a judgement based on the ranking of the rotational vibration performance number of the different CVT fluids tested is being justified to discriminate between these fluids.

In order to cover a wider range of operating conditions an extension of the test settings is being foreseen in future.

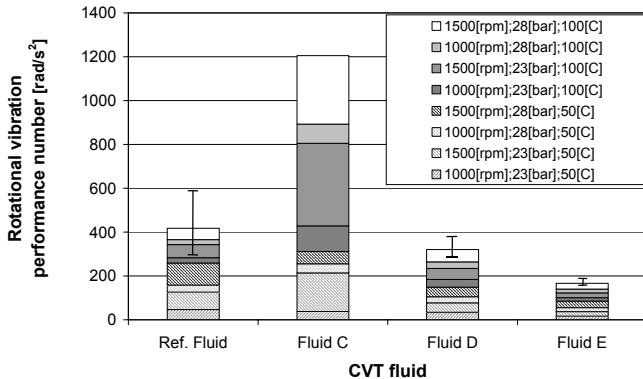


Figure 4.6.6 Rotational vibration sensitivity test fluid comparison

4.7 COOLING PROPERTIES/HEAT DISSIPATION

During variator operation heat is being dissipated in all belt-pulley contacts and internal belt contacts due to friction (frictional losses). Heat dissipation will thus depend on the coefficients of friction in the relevant contacts that are in turn influenced by the applied CVT fluids. Heat dissipation and cooling properties should therefore be considered as a potentially relevant fluid test item. However, measurement of heat dissipation/cooling properties with the current fluid test equipment is complicated.

During fluid testing the sump temperature is 100°C and the belt splash temperature is being maintained at 135(±5)°C by adjusting the belt lubrication flow. The flow that is necessary to maintain the specified splash temperature depends on the amount of heat that is being dissipated, the thermal conductivity of the fluid, but also on other factors like e.g. the temperature of the test surrounding. Even when it is being assumed that the thermal conductivity (cooling properties) of CVT fluids is quite comparable, the lubrication flow is no reliable indicator for heat dissipation due to the unknown influence of the test surrounding and so on. The measurement of coefficients of friction may however be regarded as indicative for heat dissipation.

5 CONCLUSION

- A method is being developed to test CVT fluids on a belt-pulley level. This Van Doorne CVT Fluid Test comprises full load testing in several ratios of the push belt variator at which durability and functionality related push belt CVT items are being examined.
- This Van Doorne CVT Fluid Test should be regarded as a screening test to determine the suitability of fluids for push belt CVT applications. Fluid approval/release will still require additional validation tests like Long Durability Cycles at customer specific belt boxes and testing at transmission level.
- The future goal is to develop the Van Doorne CVT Fluid Test in order to make it suitable for variator validation as part of fluid standards for CVT applications like e.g. the DEX-CVT® specification.

REFERENCES

1. Brandsma, A., van Lith, J., Hendriks, E., "Push belt CVT developments for high power applications", Proc. of CVT99, Eindhoven University of Technology 1999, pp.142-147.
2. Van der Sluis, F., Brandsma, A., van Lith, J., van der Meer, K., van der Velde, A., Pennings, B., "Stress reduction in push belt rings using residual stresses", Proc. of CVT2002 Congress, VDI-Berichte 1709, Munich, October 2002, pp.383-402.
3. Morgan, C., Fewkes, R., Marty, S.D., "Development of a belt CVT fluid test procedure using the VT20/25E belt box for the DEX-CVT® specification", SAE Technical Paper Series 2002-01-2819, 2002.
4. DIN 50320: Verschleiß – Begriffe, Systemanalyse von Verschleißvorgängen, Gliederung des Verschleißgebietes, Beuth Verlag, Berlin, 1979.
5. Larsen, R.J., Marx, M.L., "An introduction to mathematical statistics and its applications", second edition, Prentice-Hall, Englewood Cliffs, New Jersey, 1986.
6. Kobayashi, D., Mabuchi, Y. and Katoh, Y., "A Study on the Torque Capacity of a Metal Pushing V-belt for CVTs", SAE Paper 980822, 1998.
7. Rooij, J. van, Schaerlaeckens, W., "Kräfte und Wirkungsgrad beim Schubgliederband, Teil 1: Allgemeine Kräftebetrachtungen", Antriebstechnik 32 no. 8, 1993.
8. Fewkes, R., Gusing, J., Sumiejski, J.L., "Lubricant as a Construction Element in VDT Push-Belt CVT System", SAE Paper 932848, 1993.

9. Ward, W.C. jr., Kojima, N., "North American ATF Trends and Performance of CVT Fluids", JSAE Paper 9736168, 1997.
10. C.-H. Lang, J. Rach and G. Lechner, "Modellierung der Klapper- und Rasselschwingungen in Fahrzeuggetrieben", VDI Berichte Nr. 1220, 1995.
11. Bhushan, B., "Principles and applications of tribology", J. Wiley & Sons, New York, 1999.
12. D.J. Schipper, "Transitions in the lubrication of concentrated contacts", Ph.D. thesis, University of Twente, 1988.

APPENDIX

Table 2 Settings for the fixed ratio durability tests.

		TOP	OD	LOW	LOW
Test duration	[hrs]	40	40	15	20
Ratio	[-]	0.6	0.445	2.47	2.47
Primary torque	[Nm]	140	155	72.5	145
Primary speed	[rpm]	6000	4000	4000	4000
Primary pressure	[bar]	9.9	11.1	0	0
Secondary pressure	[bar]	9.9	11.1	34.6	34.6
Sump temperature	[°C]	100	100	100	100
Belt splash temperature	[°C]	135 (±5)	135 (±5)	≤135 (±5)	135 (±5)
Belt lubrication flow	[ltr/min]	> 1.5	> 1.5	> 1.5	> 1.5

Table 3 Settings for the torque capacity measurements.

		TOP	OD	OD	OD	LOW
Ratio	[-]	0.6	0.445	0.445	0.445	2.47
Primary speed	[rpm]	6000	4000	5300	4000	4000
Primary pressure	[bar]	9.9	11.1	9.2	11.1	0
Secondary pressure	[bar]	9.9	11.1	8.2	11.1	34.6
Sump temperature	[°C]	100	100	100	60	100
Belt splash temperature	[°C]	135 (±5)	135 (±5)	135 (±5)	95 (±5)	135 (±5)
Belt lubrication flow	[ltr/min]	> 1.5	> 1.5	> 1.5	> 1.5	> 1.5

Table 4 Settings for the transition torque measurements in LOW.

		LOW	LOW	LOW	LOW	LOW	LOW
Ratio	[-]	2.47	2.47	2.47	2.47	2.47	2.47
Primary speed	[rpm]	1000	1000	4000	4000	6000	6000
Primary pressure	[bar]	0	0	0	0	0	0
Secondary pressure	[bar]	34.7	34.7	34.6	34.6	34.4	34.4
Sump temperature	[°C]	60	100	60	100	60	100
Belt splash temperature	[°C]	95 (±5)	135 (±5)	95 (±5)	135 (±5)	95 (±5)	135 (±5)
Belt lubrication flow	[ltr/min]	> 1.5	> 1.5	> 1.5	> 1.5	> 1.5	> 1.5

Table 5 Settings for the rotational vibration sensitivity measurements

		LOW	LOW	LOW	LOW	LOW	LOW	LOW	LOW
Ratio	[-]	2.47	2.47	2.47	2.47	2.47	2.47	2.47	2.47
Primary speed	[rpm]	1000	1500	1000	1500	1000	1500	1000	1500
Primary pressure	[bar]	0	0	0	0	0	0	0	0
Secondary pressure	[bar]	23	28	23	28	23	28	23	28
Sump temperature	[°C]	50	50	50	50	100	100	100	100
Belt splash temperature	[°C]	n.a.	n.a.	n.a.	n.a.	n.a.	n.a.	n.a.	n.a.
Belt lubrication flow	[ltr/min]	1.5	1.5	1.5	1.5	1.5	1.5	1.5	1.5